The following publication J. Li, Z. Xu, J. Zhao and C. Zhang, "Distributed Online Voltage Control in Active Distribution Networks Considering PV Curtailment," in IEEE Transactions on Industrial Informatics, vol. 15, no. 10, pp. 5519-5530, Oct. 2019 is available at https://doi.org/10.1109/TII.2019.2903888.

Distributed Online Voltage Control in Active Distribution Networks Considering PV Curtailment

Jiayong Li, *Member, IEEE*, Zhao Xu, *Senior Member, IEEE*, Jian Zhao, and Chaorui Zhang

***Abstract*—In this paper, we propose a distributed online voltage control algorithm for distribution networks with multiple photovoltaic (PV) systems based on dual ascent method. Conventional distributed algorithms implement voltage control only when the algorithms converge. However, our proposed algorithm is able to carry out voltage control immediately. In particular, we derive a closed-form solution for PV controllers to locally update the active and reactive power set-points aiming at minimizing the total loss and maintaining bus voltages within the acceptable ranges. The optimality is guaranteed and the convergence is established analytically. Moreover, our proposed algorithm only requires the information exchange between neighboring PV systems, thus reducing communication complexity. Finally, numerical tests on IEEE 37-bus distribution system verify the effectiveness and robustness of our proposed algorithm.**

***Index Terms*—Distribution networks, photovoltaic (PV) system, distributed algorithm, online voltage control, dual ascent method.**

I. Introduction

In 2016, the total installed solar photovoltaic (PV) capacity has increased by 97%, driven by the increasing environment concerns, falling manufacturing costs and steady government incentives [1]–[3]. However, the proliferation of PV generations poses significant challenges to the operations of power systems, especially for the low-voltage distribution networks (DNs) [4]. In particular, the fast varying solar energy could result in unexpected voltage violations, at a time scale that is not consistent with conventional voltage control using on-load tap changers, step voltage regulators and shunt capacitors [5]. In this regard, PV systems can play an important role to provide voltage support in DNs [6]. Therefore, it is necessary to develop an online control scheme for dispersed PV systems to address the rapid voltage fluctuations.

Different voltgage control strategies using distributed generators (DGs) have been proposed, which can be classified into three categories, i.e. centralized strategy (e.g., [6]–[8]), decentralized strategy (e.g. [9], [10]), and distributed strategy (e.g. [11]–[13]). Under centralized voltage control, multiple DGs are dispatched centralizedly by DN operator. Centralized control is effective for relatively long term operations (e.g. hourly), but it is hard to deal with real-time operation due to its complex communication and control schemes [14]. Furthermore, it is not robust when subjected to a single point failure [12].

Under decentralized voltage control, DGs are locally managed by their own controllers instead of a central one. Generally, decentralized control includes local control and distributed control. Here it particularly refers to the former. Decentralized control, e.g., droop control, only relies on local measurements without any communication. Thus, it has much lower computational complexity compared with centralized voltage control. However, it often results in suboptimality due to the lack of coordination [14].

Under distributed control, DGs cooperate with each other to achieve a global goal predetermined by system operator or DG owners, and only communication among DGs is required [14]. A research summary on distributed voltage control for DNs can be found in [14]. Therein, dual-decomposition techniques, e.g., dual-ascent method and alternating direction method of multipliers (ADMM), are mostly used to develop distributed algorithms. For example, dual ascent method is employed in [15] to decompose a semi-definite programming (SDP) relaxed optimal power flow (OPF) problem into subproblems such that it can be solved in a distributed manner. In [13], an OPF problem that optimizes the active and reactive power set-points of PV inverters is decomposed based on ADMM and SDP relaxation. ADMM is also combined with second-order cone programming (SOCP) relaxation, to develop distributed algorithms for voltage control problem in [11], [12]. The general framework of such kind of distributed voltage control for DGs is illustrated in Fig. 1(a). It shows that multiple SDP/SOCP subproblems have to be solved iteratively before applying the final converged solution to DGs in voltage control. Consequently, the response speed of DGs cannot catch up with the fast variations of system condition, which thwarts an online application.

Apart from duality-based methods, approaches like gradient/subgradient method [16] and heuristic algorithms [17], [18] have been applied to derive distributed control schemes as well. For example, a gradient based distributed algorithm is proposed in [16] to minimize the voltage deviations in a microgrid with a consensus on reactive power utilization. In [5], a local reactive power control framework is developed to minimize the weighted voltage mismatch based on gradient-projection method. However, these strategies will inevitably encounter some problems when the reactive power capacities of inverters are insufficient, especially during peak irradiance

This work was partially supported by Hong Kong RGC Theme Based Research Scheme under Grants No. T23-407/13N and T23-701/14N and partially supported by Hong Kong RGC GRF under Grant No. 152443/16E.

J. Li is with the College of Electrical and Information Engineering, Hunan University, Changsha 410082, China, and also with the Hunan Key Laboratory of Intelligent Information Analysis and Integrated Optimization for Energy Internet, Hunan University, Changsha 410082, China, and also with the Department of Electrical Engineering, The Hong Kong Polytechnic University, Hung Hom, Hong Kong. (email: j-y.li@connect.polyu.hk).

Z. Xu is with the Department of Electrical Engineering, The Hong Kong Polytechnic University, Hung Hom, Hong Kong. (email: eezhaoxu@polyu.edu.hk).

J. Zhao is with the College of Electrical Engineering, Shanghai University of Electric Power, Shanghai 200090, China. (email: zhaojianee@foxmail.com).

C. Zhang is with the Department of Information Engineering, the Chinese University of Hong Kong, Hong Kong (e-mail: chaorui.zhang@gmail.com).

© 2019 IEEE. Personal use of this material is permitted. Permission from IEEE must be obtained for all other uses, in any current or future media, including reprinting/republishing this material for advertising or promotional purposes, creating new collective works, for resale or redistribution to servers or lists, or reuse of any copyrighted component of this work in other works.

period. In such case, PV active power has to be curtailed for ensuring the voltages within the acceptable ranges.

In this paper, we propose an efficient distributed online voltage control algorithm using dual ascent method. PV curtailment is taken into account to overcome the aforementioned inadequacy of reactive power capacity. The objective is to maintain the voltages within the acceptable ranges and meanwhile minimize the total loss consisting of network loss and PV curtailment. In our proposed algorithm, the active and reactive power (P-Q) set-points of multiple PV systems can be updated in a distributed manner based on local voltage measurements and communications between neighboring PV systems. The contributions of this paper are summarized as below.

- Different from most existing works (e.g. [11]–[13]), our proposed distributed voltage control algorithm can be implemented online. That is, each update obtained by our proposed algorithm can be applied directly into voltage control, as shown in Fig. 1(b). Therefore, the response speed is faster than conventional algorithms, where the voltage control cannot be implemented before algorithms converge. Numerical results show the voltage violations can be eliminated with only one iteration.
- We derive a closed-form solution for PV controllers to locally update P-Q set-points rather than solving SDP/SOCP subproblems in conventional algorithms. The convergence is established analytically. To speed up the convergence, the step sizes are diagonally scaled. Moreover, the optimality is guaranteed. Numerical results show our method achieves a near-optimality ($< 4\%$) of a benchmark centralized optimization problem.
- We significantly reduce the communication complexity through the analysis of the distribution network property. Consequently, each PV system only needs to communicate with its neighbors to update its P-Q set-points.
- We conduct a comprehensive sensitivity analysis to demonstrate the influence of various parameters on the voltage control and loss minimization of our proposed method. In addition, we validate its robustness against communication interruptions.

The remainder of this paper is organized as follows. Section II introduces the system model and some preliminaries. In Section III, the problem formulation is elaborated in a centralized model. In Section III, a distributed algorithm is developed based on dual ascent method. Section V demonstrates the numerical results. Finally, Section VI concludes the paper and guides our future work.

II. System Model And Preliminaries

A. System Model

Consider a radial distribution network represented by a directed tree $\mathcal{G} = (\mathcal{N},\ \mathcal{E})$, where $\mathcal{N} := \{0, 1, \ldots, N\}$ denotes the bus set and $\mathcal{E}$ denote the line set. Each bus i except the substation bus (indexed as 0) has a unique parent bus π_i and several child buses, denoted by C_i. Without loss of generality, we label the bus in a way such that $\pi_i < i$. In addition, we assume each line points from a parent node π_i to a node i and uniquely label the line as i. Hence, the label of the line is consistent with the label of the bus and $\mathcal{E} := \{1, \ldots, N\}$. Let $\mathbf{A}^0$ of size $N \times (N+1)$ denote the incidence matrix of $\mathcal{G}$, whose entries are defined as

$$A^0_{ij} = \begin{cases} 1 & \text{line } i \text{ leaves bus } j \\ -1 & \text{line } i \text{ enters bus } j \\ 0 & \text{otherwise} \end{cases}$$

Since $\mathcal{G}$ is a connected tree, the rank of $\mathbf{A}^0$ equals to N [19]. Let $\mathbf{a}_0$ denote the first column of $\mathbf{A}^0$ and $\mathbf{A}$ be the rest of $\mathbf{A}^0$, i.e. $\mathbf{A}^0 = [\mathbf{a}_0\ \mathbf{A}]$. Note that $\mathbf{A}$ is a full-rank square matrix and thus invertible.

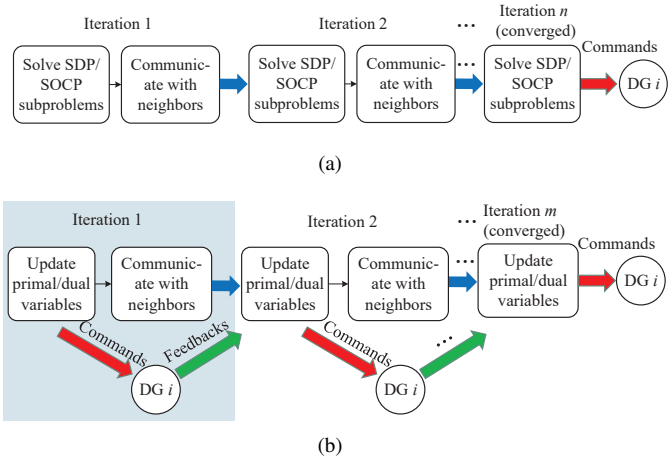

Fig. 1. (a) General distributed voltage control v.s. (b) our proposed distributed online voltage control

B. Branch Flow Model

For radial DNs, branch flow model is well established to represent the power flow equations [20] as (1a)-(1c)

$$P_i - \frac{P_i^2 + Q_i^2}{V_{\pi_i}^2} r_i + p_i = \sum_{j \in C_i} P_j \quad \forall i \in \mathcal{N}/0 \tag{1a}$$

$$Q_i - \frac{P_i^2 + Q_i^2}{V_{\pi_i}^2} x_i + q_i = \sum_{j \in C_i} Q_j \quad \forall i \in \mathcal{N}/0 \tag{1b}$$

$$V_{\pi_i}^2 - V_i^2 = 2\left(r_i P_i + x_i Q_i\right) - \left(r_i^2 + x_i^2\right) \frac{P_i^2 + Q_i^2}{V_{\pi_i}^2} \quad \forall i \in \mathcal{E} \tag{1c}$$

where p_i and q_i are active and reactive power injection at bus i; P_i and Q_i are active and reactive power flow on line i observed from the sending bus π_i; r_i and x_i are resistance and reactance of line i; V_i is voltage magnitude at bus i. Eq. (1a) and (1b) describe the active and reactive power balance at bus i, respectively. Eq. (1c) shows the voltage relationship between two neighboring buses.

Since the original branch flow model (1a)-(1c) is non-convex, linearized branch flow model (LinDistFlow) will be adopted by neglecting the high order terms and assuming a relatively flat voltage profile, i.e. $V_i \approx 1,\ \forall i$. It has been

widely used to solve DN operation and planning problems (e.g., [5], [7]) and is given by

$$P_i - \sum_{j \in C_i} P_j = -p_i \quad \forall i \in \mathcal{N}/0 \tag{2a}$$

$$Q_i - \sum_{j \in C_i} Q_j = -q_i \quad \forall i \in \mathcal{N}/0 \tag{2b}$$

$$V_{\pi_i} - V_i = r_i P_i + x_i Q_i \quad \forall i \in \mathcal{E} \tag{2c}$$

C. PV Inverter Control Strategies

Advance control strategies, e.g., optimal inverter dispatch [6], enable PV inverters to adjust both active and reactive power to provide voltage regulation service. Let p_i^m denote the maximum available active power for PV system *i*. The operating region of P-Q set-points can be represented by

$$0 \le p_i^s \le p_i^m \tag{3a}$$

$$|q_i^s| \le \sqrt{S_i^2 - \left(p_i^s\right)^2} \tag{3b}$$

where p_i^s and q_i^s are active and reactive power set-points; S_i is the rated apparent power. In order to decouple the correlation between active and reactive power, (3b) is linearized by imposing restricted limits on q_i^s as (4).

$$\underline{q}_i \le q_i^s \le \overline{q}_i \tag{4}$$

where $\overline{q}_i = \sqrt{S_i^2 - \left(p_i^m\right)^2}$ and $\underline{q}_i = -\overline{q}_i$.

III. Problem Formulation

A. Objective Function

The objective is to minimize the total loss consisting of network loss and PV curtailment cost.

The network loss is given by

$$\text{Loss} = \sum_{\forall i \in \mathcal{E}} r_i \frac{P_i^2 + Q_i^2}{V_{\pi_i}^2} \approx \sum_{\forall i \in \mathcal{E}} r_i \frac{P_i^2 + Q_i^2}{V_0^2} \tag{5}$$

where V_0 is the voltage magnitude at the substation bus and is assumed to be 1 p.u. without loss of generality; V_{π_i} is approximated by V_0 since $V_i \approx 1,\ \forall i$.

PV curtailment cost is evaluated by a convex quadratic function, which is given as

$$h\left(\mathbf{p}^c\right) = K \cdot \left(\mathbf{p}^c\right)^T \mathbf{R} \mathbf{p}^c \tag{6}$$

where $\mathbf{p}^c$ is the vector collecting all p_i^c and p_i^c is curtailment amount of PV system *i*; $\mathbf{R}$ is a positive definite matrix with positive entries, which will be further explained in subsection III-C. Thus, $h\left(\mathbf{p}^c\right)$ is strictly increasing in each component of $\mathbf{p}^c$. K is an adjustable parameter. A larger K results in less PV curtailment amount but lower efficiency in eliminating overvoltage violations, vice versa.

Hence, the total loss is given as

$$F = \text{Loss} + h\left(\mathbf{p}^c\right) \tag{7}$$

B. Constraints

The constraints include power flow equations, voltage constraints and PV operation constraints. The power flow equations are represented by LinDistFlow model as (8)-(10)

$$(2a)\text{-}(2c) \tag{8}$$

$$p_i = p_i^m - p_i^c - p_i^l \quad \forall i \in \mathcal{N}/0 \tag{9}$$

$$q_i = q_i^s - q_i^l \quad \forall i \in \mathcal{N}/0 \tag{10}$$

where p_i^l and q_i^l are active and reactive load at bus i. The PV system located at bus i is labelled as PV i so that the indices of PV systems are identical with the indices of buses.

The bus voltage magnitudes should be maintained within the acceptable ranges as

$$\underline{V}_i \le V_i \le \overline{V}_i \quad \forall i \in \mathcal{N}/0 \tag{11}$$

where $\underline{V}_i$ and $\overline{V}_i$ are the lower and upper limits for V_i.

PV active power curtailment and reactive power set-point are constrained by

$$0 \le p_i^c \le p_i^m \quad \forall i \in \mathcal{N}/0 \tag{12}$$

$$\underline{q}_i \le p_i^s \le \overline{q}_i \quad \forall i \in \mathcal{N}/0 \tag{13}$$

C. Centralized Optimization Model

The centralized optimization model is given as

$$\text{CEN1} \qquad \min_{p_i^c, q_i^s} \ F = \text{Loss} + h\left(\mathbf{p}^c\right)$$
$$\text{s.t. } (8)\text{-}(13)$$

CEN1 is a convex quadratic optimization problem with linear constraints. A distributed online algorithm will be developed in the next section to solve it. Towards this end, it will be written in a compact matrix format for clarity. The corresponding compact form for LinDistFlow model is given as

$$-\mathbf{A}^T \mathbf{P} = -\mathbf{p} \tag{14a}$$

$$-\mathbf{A}^T \mathbf{Q} = -\mathbf{q} \tag{14b}$$

$$\mathbf{a}_0 + \mathbf{A}\mathbf{V} = \mathbf{D}_r \mathbf{P} + \mathbf{D}_x \mathbf{Q} \tag{14c}$$

$$\mathbf{p} = \mathbf{p}^m - \mathbf{p}^c - \mathbf{p}^l \tag{14d}$$

$$\mathbf{q} = \mathbf{q}^s - \mathbf{q}^l \tag{14e}$$

where $\mathbf{D}_r$ and $\mathbf{D}_x$ are $N \times N$ diagonal matrices whose diagonal entries are constituted by r_i and x_i, respectively. Solving $\mathbf{P}$ and $\mathbf{Q}$ and plugging them into (14c), LinDistFlow model boils down to

$$\mathbf{V} = \mathbf{R}\mathbf{p} + \mathbf{X}\mathbf{q} + V_0 \mathbf{1} \tag{15}$$

where $\mathbf{R} := \mathbf{A}^{-1}\mathbf{D}_r\mathbf{A}^{-T}$, $\mathbf{X} := \mathbf{A}^{-1}\mathbf{D}_x\mathbf{A}^{-T}$ and $\mathbf{1}$ is a N demension vector with the value of each component being 1. Eq. (15) reveals linear relationship between nodal power injections and bus voltage magnitudes. According to Proposition 1 in [5], $\mathbf{R}$ and $\mathbf{X}$ are positive definite (PD) and their entries are positive.

The network loss can be reformulated as

$$\begin{aligned} \text{Loss} &= \sum_{\forall i \in \mathcal{E}} \left[\left(\sqrt{r_i} P_i\right)^2 + \left(\sqrt{r_i} Q_i\right)^2 \right] \\ &= \|\mathbf{D}_r^{1/2}\mathbf{P}\|_2^2 + \|\mathbf{D}_r^{1/2}\mathbf{Q}\|_2^2 = \mathbf{p}^T\mathbf{R}\mathbf{p} + \mathbf{q}^T\mathbf{R}\mathbf{q} \end{aligned} \tag{16}$$

$$\begin{aligned}\mathcal{L} =& \frac{K+1}{2}\left(\mathbf{p}^c\right)^T\mathbf{R}\mathbf{p}^c - \left(\mathbf{p}^m-\mathbf{p}^l\right)^T\mathbf{R}\mathbf{p}^c + \frac{1}{2}\left(\mathbf{q}^s\right)^T\mathbf{R}\mathbf{q}^s - \left(\mathbf{q}^l\right)^T\mathbf{R}\mathbf{q}^s + \underline{\boldsymbol{\mu}}^T\left(\underline{\mathbf{V}}+\mathbf{R}\mathbf{p}^c-\mathbf{X}\mathbf{q}^s-\mathbf{V}^r\right)\\ &+\overline{\boldsymbol{\mu}}^T\left(-\overline{\mathbf{V}}-\mathbf{R}\mathbf{p}^c+\mathbf{X}\mathbf{q}^s+\mathbf{V}^r\right)+\underline{\boldsymbol{\nu}}^T(\mathbf{0}-\mathbf{p}^c)+\overline{\boldsymbol{\nu}}^T(\mathbf{p}^c-\mathbf{p}^m)+\underline{\boldsymbol{\omega}}^T(\underline{\mathbf{q}}-\mathbf{q}^s)+\overline{\boldsymbol{\omega}}^T(\mathbf{q}^s-\overline{\mathbf{q}})\end{aligned} \tag{20}$$

The last equality follows from the substitution of $\mathbf{P}$ and $\mathbf{Q}$. Note that the PV curtailment evaluation in (6) shares a similar structure with the network loss in (16). It will be demonstrated in the next section that such a modelling of PV curtailment will facilitate the reduction of communication complexity.

By plugging (14d) and (14e) into (15) and (16), we obtain the compact format of CEN1 as

$$\begin{aligned}\min_{\mathbf{p}^c,\mathbf{q}^s}\ & \frac{1}{2}\Big[\left(\mathbf{p}^m-\mathbf{p}^c-\mathbf{p}^l\right)^T\mathbf{R}\left(\mathbf{p}^m-\mathbf{p}^c-\mathbf{p}^l\right)\\ &+\left(\mathbf{q}^s-\mathbf{q}^l\right)^T\mathbf{R}\left(\mathbf{q}^s-\mathbf{q}^l\right)\Big]+\frac{K}{2}\left(\mathbf{p}^c\right)^T\mathbf{R}\mathbf{p}^c && \text{(17a)}\\ \text{s.t. }& \mathbf{V}=\mathbf{R}\left(\mathbf{p}^m-\mathbf{p}^c-\mathbf{p}^l\right)+\mathbf{X}\left(\mathbf{q}^s-\mathbf{q}^l\right)+V_0\mathbf{1} && \text{(17b)}\\ & \underline{\mathbf{V}}\le\mathbf{V}\le\overline{\mathbf{V}} && \text{(17c)}\\ & \mathbf{0}\le\mathbf{p}^c\le\mathbf{p}^m && \text{(17d)}\\ & \underline{\mathbf{q}}\le\mathbf{q}^s\le\overline{\mathbf{q}} && \text{(17e)}\end{aligned}$$

IV. Distributed Online Voltage Control

A. Distributed Online Algorithm

In this subsection, we develop a distributed online algorithm using dual ascent method. In particular, a closed-form solution is derived for PV systems to locally update P-Q set-points and Lagrangian multipliers.

1) Dual Ascent Method: In dual ascent method [21], the dual problem is solved using gradient projection algorithm and the primal optimal solution is recovered from the dual optimal solution. Define the dual problem as $\mathcal{D}(\mathbf{y})=\min_{\mathbf{x}}\mathcal{L}(\mathbf{x},\mathbf{y})$, where $\mathcal{L}(\mathbf{x},\mathbf{y})$ is the Lagrangian function. The iterations of Lagrangian multipliers $\mathbf{y}$ and primal variables $\mathbf{x}$ are given as (18) and (19), respectively.

$$\mathbf{y}^{k+1}=\left[\mathbf{y}^k+\alpha^k\nabla\mathcal{D}\left(\mathbf{y}^k\right)\right]^Y \tag{18}$$

$$\mathbf{x}^{k+1}=\arg\min_{\mathbf{x}}\mathcal{L}(\mathbf{x},\mathbf{y}^{k+1}) \tag{19}$$

where $\nabla\mathcal{D}\left(\mathbf{y}^k\right)$ is the gradient of the dual problem at $\mathbf{y}^k$, α^k is the step size at k-th iteration, Y is the feasible set of $\mathbf{y}$, and $[\cdot]^Y$ denotes the projection operator onto the set Y.

2) Update Rules for Lagrangian Multipliers: The Lagrangian function of CEN1 is given as (20) located at top of this paper, where $\underline{\boldsymbol{\mu}}$, $\overline{\boldsymbol{\mu}}$, $\underline{\boldsymbol{\nu}}$, $\overline{\boldsymbol{\nu}}$, $\underline{\boldsymbol{\omega}}$ and $\overline{\boldsymbol{\omega}}$ are Lagrangian multipliers associated with (17c), (17d) and (17e), respectively; and $\mathbf{V}^r:=\mathbf{R}(\mathbf{p}^m-\mathbf{p}^l)-\mathbf{X}\mathbf{q}^l+V_0\mathbf{1}$.

The Lagrangian multipliers are locally updated based on gradient projection method for each PV system [22], given as

$$\underline{\mu}_i^{k+1}=\left[\underline{\mu}_i^k+\underline{\alpha}_i(\underline{V}_i-V_i^k)\right]^+ \tag{21a}$$

$$\overline{\mu}_i^{k+1}=\left[\overline{\mu}_i^k+\overline{\alpha}_i(V_i^k-\overline{V}_i)\right]^+ \tag{21b}$$

$$\underline{\nu}_i^{k+1}=\left[\underline{\nu}_i^k+\underline{\beta}_i(0-p_i^{c,k})\right]^+ \tag{21c}$$

$$\overline{\nu}_i^{k+1}=\left[\overline{\nu}_i^k+\overline{\beta}_i(p_i^{c,k}-p_i^m)\right]^+ \tag{21d}$$

$$\underline{\omega}_i^{k+1}=\left[\underline{\omega}_i^k+\underline{\gamma}_i(\underline{q}_i-q_i^{s,k})\right]^+ \tag{21e}$$

$$\overline{\omega}_i^{k+1}=\left[\overline{\omega}_i^k+\overline{\gamma}_i(q_i^{s,k}-\overline{q}_i)\right]^+ \tag{21f}$$

where $\underline{\alpha}_i$, $\overline{\alpha}_i$, $\underline{\beta}_i$, $\overline{\beta}_i$, $\underline{\gamma}_i$ and $\overline{\gamma}_i$ are step sizes for PV i, and $[\cdot]^+$ denotes the projection operator onto the non-negative range.

3) Update Rules for Primal Variables: Since $\mathcal{L}$ is a quadratic function of $\mathbf{p}^c$ and $\mathbf{q}^s$, a closed-form solution at k-th iteration can be obtained as

$$\mathbf{p}^{c,k}=\frac{\mathbf{p}^m-\mathbf{p}^l+\overline{\boldsymbol{\mu}}^k-\underline{\boldsymbol{\mu}}^k+\mathbf{R}^{-1}(\underline{\boldsymbol{\nu}}^k-\overline{\boldsymbol{\nu}}^k)}{K+1} \tag{22a}$$

$$\mathbf{q}^{s,k}=\mathbf{q}^l+\mathbf{R}^{-1}\mathbf{X}(\underline{\boldsymbol{\mu}}^k-\overline{\boldsymbol{\mu}}^k)+\mathbf{R}^{-1}(\underline{\boldsymbol{\omega}}^k-\overline{\boldsymbol{\omega}}^k) \tag{22b}$$

The optimization problem (19) boils down to trivial algebraic operations. However, it is still unclear to see how the information is exchanged among PV systems. By using the following two propositions, we will show that each PV system only needs to exchange Lagrangian multipliers with its neighboring PV systems for the update of active power curtailment and reactive power set-point.

Proposition 1. *Denote* $\mathbf{H}:=\mathbf{R}^{-1}:=\mathbf{A}^T\mathbf{D}_r^{-1}\mathbf{A}$. $\mathbf{H}$ *is a weighted Laplacian matrix induced by the network incidence matrix* $\mathbf{A}$. *For any pair of buses* (i,j) *that are not directly connected, the corresponding entry is zero, i.e.* $(i,j)\notin\mathcal{E}\Leftrightarrow H_{ij}=0$.

The proof of Proposition 1 is deferred to Appendix A.

Proposition 2. *The* i*-th component of* $\mathbf{R}^{-1}\mathbf{X}(\underline{\boldsymbol{\mu}}^k-\overline{\boldsymbol{\mu}}^k)$ *only involves the information of PV system* i *and PV systems on its child buses* C_i.

Proof. Plugging $\mathbf{R}$ and $\mathbf{X}$, $\mathbf{R}^{-1}\mathbf{X}(\underline{\boldsymbol{\mu}}^k-\overline{\boldsymbol{\mu}}^k)$ is transformed to

$$\mathbf{R}^{-1}\mathbf{X}(\underline{\boldsymbol{\mu}}^k-\overline{\boldsymbol{\mu}}^k)=\mathbf{A}^T\mathbf{D}_{\frac{x}{r}}(\underline{\boldsymbol{\lambda}}^k-\overline{\boldsymbol{\lambda}}^k) \tag{23}$$

where $\mathbf{D}_{\frac{x}{r}}:=\mathbf{D}_r^{-1}\mathbf{D}_x$, $\underline{\boldsymbol{\lambda}}^k:=\mathbf{A}^{-T}\underline{\boldsymbol{\mu}}^k$ and $\overline{\boldsymbol{\lambda}}^k:=\mathbf{A}^{-T}\overline{\boldsymbol{\mu}}^k$. By observing Eq.(2a) and (14a), we have

$$\overline{\lambda}_i^k=\sum_{j\in Ci}\overline{\lambda}_j^k-\overline{\mu}_i^k \tag{24a}$$

$$\underline{\lambda}_i^k=\sum_{j\in Ci}\underline{\lambda}_j^k-\underline{\mu}_i^k \tag{24b}$$

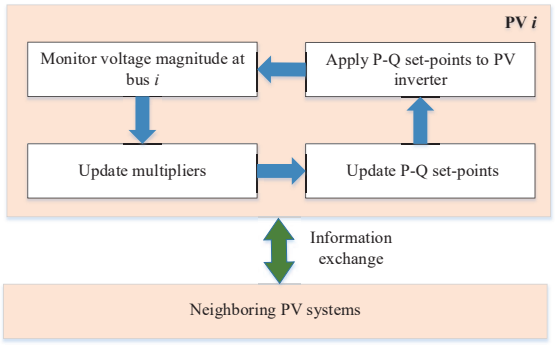

Fig. 2. One iteration of the proposed distributed voltage control algorithm for online implementation

Hence, each PV system i only needs to know $\overline{\lambda}_j^k$ and $\underline{\lambda}_j^k$ of PV systems on its child buses for calculating $\overline{\lambda}_i^k$ and $\underline{\lambda}_i^k$. Expanding (23), we can obtain the i-th component of $\mathbf{R}^{-1}\mathbf{X}(\underline{\boldsymbol{\mu}}^k - \overline{\boldsymbol{\mu}}^k)$ as

$$\left[\mathbf{R}^{-1}\mathbf{X}(\underline{\boldsymbol{\mu}}^k - \overline{\boldsymbol{\mu}}^k)\right]_i = -\frac{x_i}{r_i}(\underline{\lambda}_i^k - \overline{\lambda}_i^k) + \sum_{j\in Ci}\frac{x_j}{r_j}(\underline{\lambda}_j^k - \overline{\lambda}_j^k)$$

Therefore, $\left[\mathbf{R}^{-1}\mathbf{X}(\underline{\boldsymbol{\mu}}^k - \overline{\boldsymbol{\mu}}^k)\right]_i$ only involves $\underline{\lambda}_i^k, \overline{\lambda}_i^k$ and $\underline{\lambda}_j^k, \overline{\lambda}_j^k$, where j is the index of child buses of bus i. □

Applying (22) to a particular PV system i, we have

$$p_i^{c,k} = \frac{p_i^m - p_i^l + \overline{\mu}_i^k - \underline{\mu}_i^k + H_{ii}(\underline{\nu}_i^k - \overline{\nu}_i^k) + \sum_{j\in\mathcal{N}_i} H_{ij}(\underline{\nu}_j^k - \overline{\nu}_j^k)}{K+1} \tag{25a}$$

$$q_i^{s,k} = q_i^l - \frac{x_i}{r_i}(\underline{\lambda}_i^k - \overline{\lambda}_i^k) + \sum_{j\in Ci}\frac{x_j}{r_j}(\underline{\lambda}_j^k - \overline{\lambda}_j^k) + H_{ii}(\underline{\omega}_i^k - \overline{\omega}_i^k) + \sum_{j\in\mathcal{N}_i} H_{ij}(\underline{\omega}_j^k - \overline{\omega}_j^k) \tag{25b}$$

where $\mathcal{N}_i := \{\pi_i, C_i\}$ denotes the set of neighbors of PV system i. Now the update for each PV system is only coupled with its neighbors.

Since constraints (17d) and (17e) are relaxed, the primal variables obtained from (25a) and (25b) may be infeasible. In case of infeasibility, they will be projected onto the feasible ranges as

$$p_i^{c,k,a} = \left[p_i^{c,k}\right]_0^{p_i^m} \tag{26a}$$

$$q_i^{s,k,a} = \left[q_i^{s,k}\right]_{\underline{q}_i^k}^{\overline{q}_i^k} \tag{26b}$$

where $[\cdot]_a^b$ denotes the projection operator onto the range $[a,b]$; $\overline{q}_i^k$ and $\underline{q}_i^k$ are iteratively renewed as $\overline{q}_i^k = \sqrt{S_i^2 - (p_i^m - p_i^{c,k,a})^2}$ and $\underline{q}_i^k = -\overline{q}_i^k$. Compared with the fixed limits in (17e), $\overline{q}_i^k$ and $\underline{q}_i^k$ enlarge the reactive power capacity and thereby improving the system performance as will be shown in Section V.

4) Implementation of the Distributed Algorithm: Fig. 2 shows one iteration of the proposed distributed algorithm for online implementation and Fig. 3 illustrates the information exchange between neighboring PV systems, where π_i and j denote the parent bus and child bus of bus i, respectively. We assume each bus is equipped with a PV system that could monitor the local bus voltage magnitude and communicate with its neighboring PV systems. Each iteration of the process consists of five steps below.

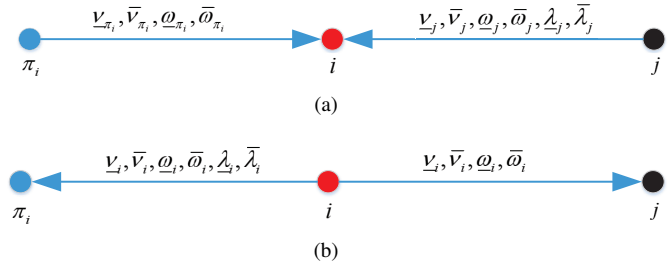

Fig. 3. Information exchange between neighboring PV systems (a) PV i receives information from its neighbors (b) PV i sends information to its neighbors

Step 1: Monitor the local bus voltage magnitude V_i.

Step 2: Update Lagrangian multipliers according to (21a)-(21f).

Step 3: Exchange multipliers with neighboring PV systems.

Step 4: Update active power curtailment and reactive power set-point according to (25a) and (25b) and project them onto the feasible ranges as (26a) and (26b).

Step 5: Apply the P-Q set-points to the PV inverter.

Since each iteration only involves simple algebraic operations and limited communication between neighboring PV system, the time required to implement the above five steps is negligibly short. Moreover, the duration of transient process is also very short. Hence, we choose a four-second duty cycle for each iteration just like the case in the automatic generation control (AGC) [23]. In other words, the iteration is repeated every four seconds until the stopping criterion is met. In this paper, the voltage stopping criterion is adopted since the optimal solution is directly related to the bus voltages. Specifically, if the voltage difference of two successive iterations is smaller than the tolerance ϵ, i.e. $|V_i^k - V_i^{k-1}| < \epsilon$, then the iteration will stop.

B. Convergence Analysis

CEN1 is a strongly convex quadratic problem with linear inequality constraints and can be written more compactly as

$$\min_{\mathbf{x}} \ \frac{1}{2}\mathbf{x}^T\mathbf{Q}\mathbf{x} + \mathbf{c}^T\mathbf{x} \tag{27a}$$

$$\text{s.t. } \mathbf{B}\mathbf{x} \le \mathbf{b} \tag{27b}$$

where $\mathbf{x}$ is the vector of decision variables collecting $\mathbf{p}^c$ and $\mathbf{q}^s$. $\mathbf{Q}$ and $\mathbf{B}$ are coefficient matrices, $\mathbf{c}$ and $\mathbf{b}$ are coefficient vectors. The strong convexity of (27) implies $\mathbf{Q}$ is PD and invertible. The associated dual problem is given by

$$\max_{\mathbf{y}\ge\mathbf{0}} \ g(\mathbf{y}) = -\frac{1}{2}\mathbf{y}^T\mathbf{B}\mathbf{Q}^{-1}\mathbf{B}^T\mathbf{y} - (\mathbf{B}\mathbf{Q}^{-1}\mathbf{c}+\mathbf{b})^T\mathbf{y} - \frac{1}{2}\mathbf{c}^T\mathbf{Q}^{-1}\mathbf{c} \tag{28}$$

where $\mathbf{y}$ is the vector of dual variables collecting $\underline{\boldsymbol{\mu}}$, $\overline{\boldsymbol{\mu}}$, $\underline{\boldsymbol{\nu}}$, $\overline{\boldsymbol{\nu}}$, $\underline{\boldsymbol{\omega}}$ and $\overline{\boldsymbol{\omega}}$. Then the update rules of dual and primal variables are given as

$$\mathbf{y}^{k+1} = \left[\mathbf{y}^k + \mathbf{D}(\mathbf{B}\mathbf{x}^k - \mathbf{b})\right]^+ \tag{29}$$

$$\mathbf{x}^{k+1} = -\mathbf{Q}^{-1}\mathbf{c} - \mathbf{Q}^{-1}\mathbf{B}^T\mathbf{y}^{k+1} \tag{30}$$

where $\mathbf{D}$ is a diagonal matrix whose diagonal entries are constituted by the step sizes.

Theorem 1. *Considering the update rules of (29) and (30), the trajectories of* $\mathbf{x}^k$ *and* $\mathbf{y}^k$ *asymptotically converge to the optimal solutions* $\mathbf{x}^*$ *and* $\mathbf{y}^*$*, respectively, if the largest eigenvalue of PD matrix* $\mathbf{D}^{\frac{1}{2}}\mathbf{B}\mathbf{Q}\mathbf{B}^T\mathbf{D}^{\frac{1}{2}}$ *is smaller than 2*

The proof of Theorem 1 is deferred to Appendix B.

V. Numerical results

In this section, we test our proposed distributed online voltage control algorithm, denoted as DIS, on the modified IEEE 37-bus distribution system. The network topology and system data can be found in [24]. The nominal voltage value is 4.8 kV and per unit value is used in the case studies. Suppose each bus except the substation bus is equipped with a PV system with 150 kW peak capacity and 1.05×150 kVA rated apparent power. Four case studies are carried out. In the first one, we apply DIS to two representative static cases and compare its performance with three other approaches. Then, we conduct a sensitivity analysis on various parameters to demonstrate their influence on voltage control and loss minimization of DIS. In the third case study, we verify the robustness of DIS against communication interruptions. Finally, we test DIS on dynamic cases of system loading and PV generation with one-minute resolution. Note that in all cases the actual bus voltage magnitudes obtained from local voltage measurements are used for updating Lagrangian multipliers . The acceptable range for bus voltage magnitudes is set as [0.95, 1.05] p.u.. All tests are implemented using MATLAB on a personal computer with an Intel Core i5 of 2.4GHz and 12GB memory.

A. Performance Comparisons

In this section, we compare the performance of DIS with two centralized strategies (CEN1 and CEN2) and a decentralized Q-V droop control scheme (Droop), where CEN1 is to solve the problem (17) in a centralized manner and CEN2 is to minimize the total loss using SOCP relaxed branch flow model. CEN2 is regardes as the benchmark. Note that here we use the standard form of linear droop VAR control method as shown by Fig. 4 and thus do not need to optimize its parameters. To speed up the convergence of DIS, the step sizes are diagonally scaled. Specifically, $\underline{\beta}_i$, $\overline{\beta}_i$, $\underline{\gamma}_i$ and $\overline{\gamma}_i$ are chosen as $0.8/H_{ii}$, where H_{ii} is i-th diagonal entry of matrix $\mathbf{H}$. $\underline{\alpha}_i$ is set as 3. $\overline{\alpha}_i$ is chosen adaptively in order to quickly eliminate overvoltage violations. If an overvoltage violation occurs, a big step size will be applied to $\overline{\alpha}_i$, e.g., 150. Otherwise, a normal step size will be applied, e.g., 50. K is set as 200.

Two representative cases corresponding to high negative net load and positive net load will be considered, as the former leads to overvoltage issues and the latter leads to undervoltage issues.

Case 1: high negative net load during the period of peak PV generation. Without loss of generality, the load at that moment is assumed to be 50% of the peak load.

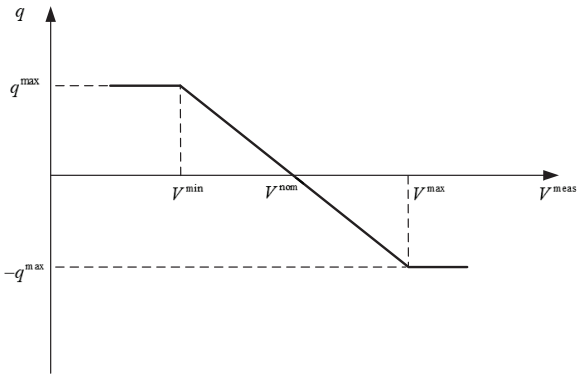

Fig. 4. Linear droop VAR control curve without deadband

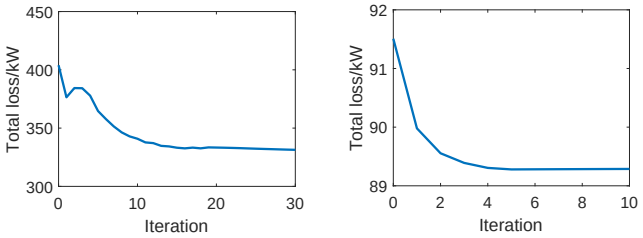

(a) case 1 (b) case 2

Fig. 5. Convergence of the total loss for (a) overvoltage case and (b) undervoltage case

Case 2: high positive net load during the period of peak load. Since the peak load often occurs at night, PV generation is not available at that moment.

Fig. 5 shows the convergence of the total loss for cases 1 and 2, representatively. It is observed that the total loss of case 1 is much higher than that of case 2. Moreover, the convergence speed in case 1 is also slower than that in case 2. The reason is that in case 1 the goal of alleviating voltage violations conflicts with the goal of reducing the total loss, while in case 2 they are consistent. Specifically, to mitigate overvoltage violations in case 1, PV systems need to increase their reactive power consumptions and reduce active power productions, which gives rise to the increase of the total loss. In contrast, in case 2, raising the reactive power productions of PV systems not only facilitates the alleviation of undervoltage violations but also contributes to the reduction of network loss. Fig. 6(a) and 6(b) depict the convergence of the maximum bus voltage magnitude for case 1 and the convergence of the minimum bus voltage magnitude for case 2, respectively. Prior to the iterations, severe overvoltage and undervoltage violations are observed in cases 1 and 2, respectively. However, the voltage violations are eliminated immediately with only one iteration in both cases using our proposed DIS and thus validating the high efficiency of DIS.

Tables I and II summarize the performance comparisons of four different approaches for cases 1 and 2, respectively, where P^{cur} and P^{loss} denote the PV curtailment and the network loss, respectively. For each method, the total loss is compared with the benchmark result, i.e. the total loss under CEN2, and the ratios to the benchmark result are exhibited in the tables. Fig. 7 and Fig. 8 plot the corresponding bus

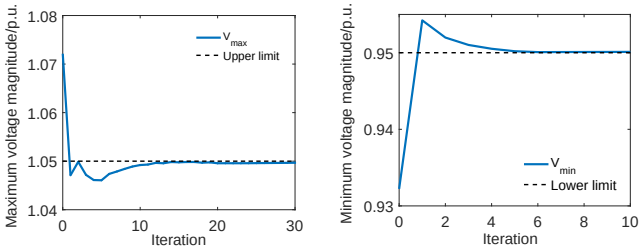

(a) case 1 (b) case 2

Fig. 6. Convergence of (a) the maximum bus voltage magnitude for overvoltage case and (b) the minimum bus voltage magnitude for undervoltage case

TABLE I
PERFORMANCE COMPARISONS OF DIFFERENT METHODS FOR CASE 1

Methods	P^{cur}/kW	P^{loss}/kW	Total loss/kW	Ratio
DIS	51.5	278.4	329.9	1.045
CEN1	154.8	273.5	428.3	1.357
CEN2	25.1	290.5	315.6	1
Droop	0	277.1	277.1	0.878

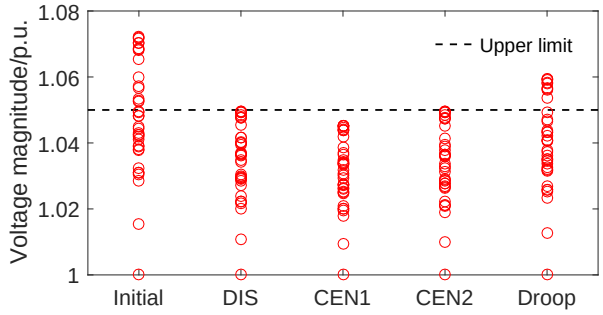

Fig. 7. Bus voltage magnitudes under different methods for case 1

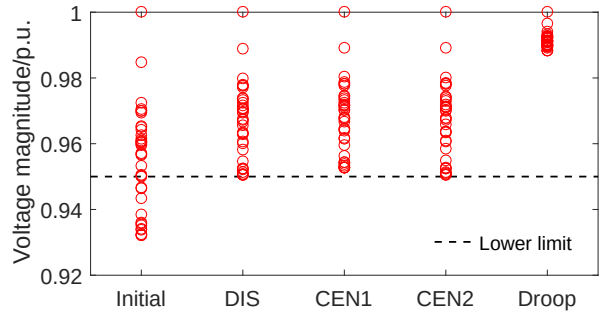

Fig. 8. Bus voltage magnitudes under different methods for case 2

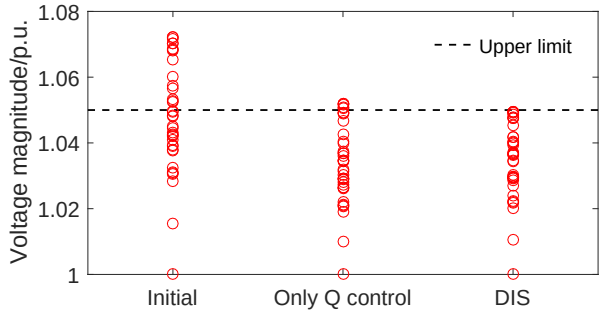

Fig. 9. Bus voltage magnitudes without and with PV curtailment

TABLE II
PERFORMANCE COMPARISONS OF DIFFERENT METHODS FOR CASE 2

Methods	P^{cur}/kW	P^{loss}/kW	Total loss/kW	Ratio
DIS	0	89.4	89.4	1.001
CEN1	0	95.3	90.3	1.011
CEN2	0	89.3	89.3	1
Droop	0	246.1	246.1	2.753

Note: oscillation is observed in Droop

voltage magnitudes under different methods, respectively. With a first glance of the results, we may conclude that in both cases CEN2 outperforms other methods in terms of voltage control and loss minimization providing that the centralized control is applicable. However, in practice, the centralized method is incapable of dealing with the real-time problem, especially the voltage problem caused by the rapid variation of PV generation, due to the considerable computational and communication burden. In contrast, our proposed method DIS can be applied online to address the real-time voltage problem. As can be observed from the results, DIS can not only efficiently remove voltage violations but also yield a relatively low total loss that is just slightly higher than the total loss using CEN2. Note although Droop is a decentralized method and can be also applied online, it fails to remove the overvoltage violations in case 1 and results in system oscillation and considerably higher network loss in case 2. The reason is that the droop method is prone to system instability as pointed out by ref [10] and it does not take network loss into consideration. Furthermore, it is interesting to notice that DIS achieves a better performance in loss minimization than CEN1, even though DIS is derived from CEN1. One reason is that in CEN1 the reactive power capacity is fixed at a restricted value, while it is iteratively renewed in DIS. Another reason is that in CEN1 the voltages are approximated using LinDistFlow model. Therein, approximation error could result in voltage violations. To avoid this kind of voltage violations, the upper and lower voltage limits in CEN1 need to be tightened, which causes additional network loss. Nevertheless, in DIS the actual voltage values obtained from local voltage measurements are used to update the multipliers and thereby avoiding approximation error. Therefore, DIS outperforms other three methods in addressing real-time voltage problem.

To demonstrate the contribution of reaction power control to the voltage regulation, we depict the bus voltage magnitudes with only reactive power control and with both active and reactive power control (DIS) in Fig. 9 along with the bus voltage magnitudes before the implementation of the control. Note that although the reactive power control can significantly mitigate the overvoltage violations, it fails to eliminate the violations without curtailing PV generation due to the limited reactive power capacity of PV inverters during the period of peak PV generation. Moreover, with the increasing adoption of PV generation, the overvoltage issue will become more severe that cannot be resolved by the reactive power control alone. Therefore, PV curtailment is necessary to address this issue.

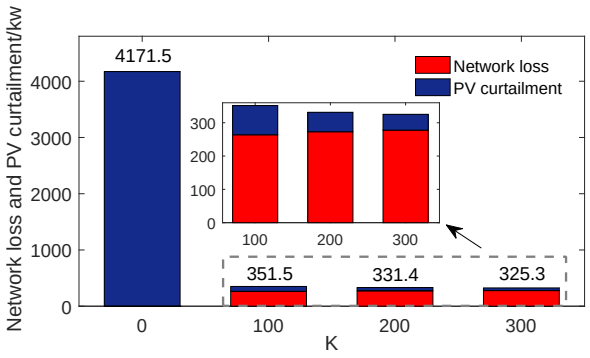

Fig. 10. Network loss and PV curtailment under different K for case 1

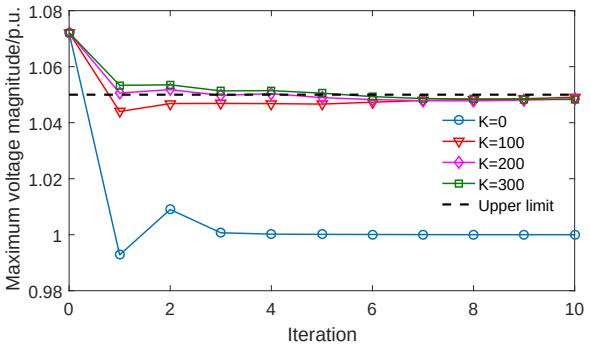

Fig. 11. Convergence of maximum voltage magnitude under different K for case 1

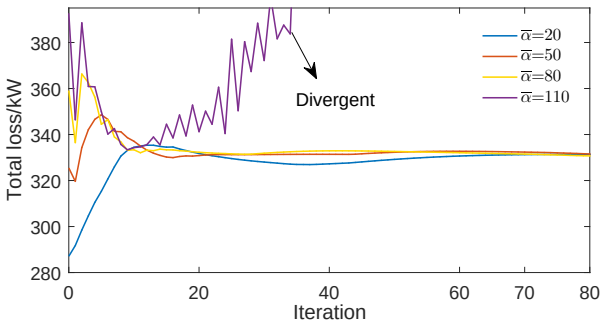

Fig. 12. Convergence of total loss under different step size $\overline{\alpha}$ for case 1

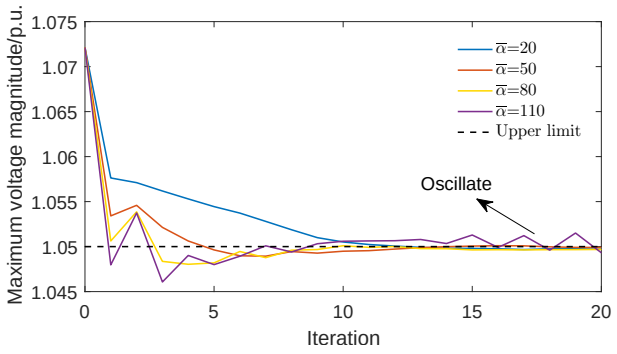

Fig. 13. Convergence of maximum voltage magnitude under different step size $\overline{\alpha}$ for case 1

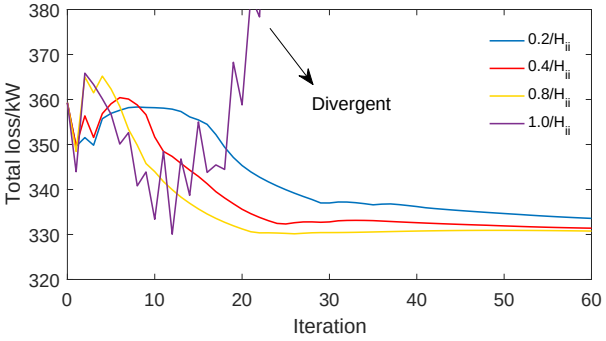

Fig. 14. Convergence of total loss under different step size $\overline{\beta}, \underline{\gamma}$ for case 1

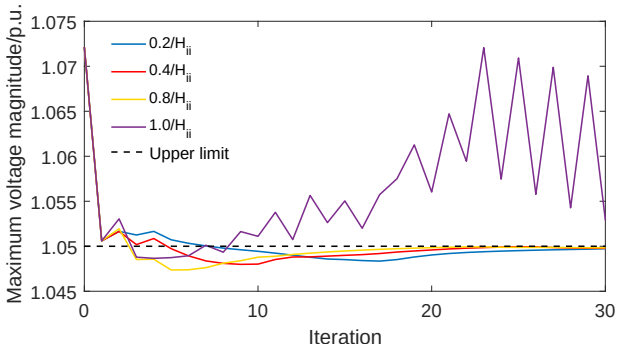

Fig. 15. Convergence of maximum voltage magnitude under different step size $\overline{\beta}, \underline{\gamma}$ for case 1

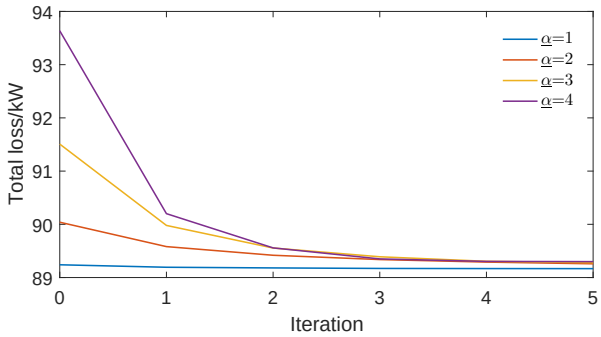

Fig. 16. Convergence of total loss under different step size $\underline{\alpha}$ for case 2

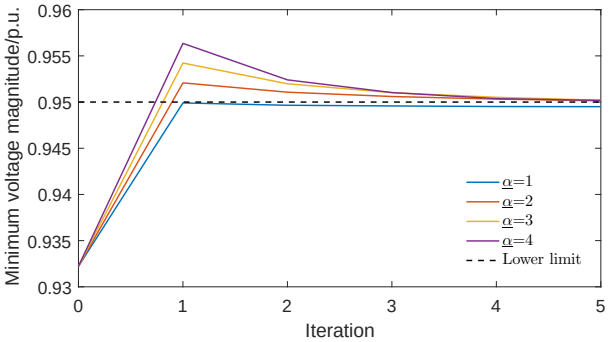

Fig. 17. Convergence of minimum voltage magnitude under different step size $\overline{\alpha}$ for case 2

B. Sensitivity analysis

In this subsection, sensitivity analysis on various parameters are conducted. Firstly, we demonstrate the influence of the parameter K on the voltage control and loss minimization of our proposed method. Fig. 10 shows the network loss and PV curtailment under different K for overvoltage case (case 1). Note that the parameter K is indifferent to the undervotlage case (case 2) since no PV curtailment is required. We can see

TABLE III
COMPARISONS OF ROBUST PERFORMANCE FOR 37-BUS SYSTEM

Probability ρ	Case1		Case2	
	Loss/kW	Iteration	Loss/kW	Iteration
0	340.9	11	89.3	7
0.1	336.6	18.4	89.3	7.2
0.2	337.8	21.6	89.3	7.4
0.3	340.2	23.5	89.3	7.1

from the figure when $K = 0$, a great amount of PV generation is curtailed since its cost is not taken into account. When K grows to 100, PV curtailment is substantially reduced. With the increase of K, PV curtailment and total loss continue to diminish. Fig. 11 depicts the convergence of the maximum bus voltage magnitude under different K for case 1. It can be seen when $K < 200$, the overvoltage violations are quickly removed with only one iteration. But when $K \geq 200$, it takes several iterations to eliminate the overvoltage violations. Hence, there is a tradeoff between minimizing the total loss and improving the voltage control performance. Tuning K to 100 is an appropriate choice for the considered case.

Secondly, we also illustrate the impact of the step sizes on the performance of DIS. Fig. 12 and Fig. 13 demonstrate the convergence of the total loss and maximum bus voltage magnitude under different $\overline{\alpha}$ for case 1, respectively. We can observe that increasing $\overline{\alpha}$ to some extent can accelerate the convergence of the total loss and voltage magnitude. But when the value of $\overline{\alpha}$ reaches 110, the algorithm fails to converge as shown by the purple curves in Fig. 12 and Fig. 13. Fig. 14 and Fig. 15 show the convergence of the total loss and maximum bus voltage magnitude under different values of $\overline{\beta}$ and $\underline{\gamma}$ for case 1, respectively. The similar phenomenon is observed and the algorithm diverges when the values of $\overline{\beta}$ and $\underline{\gamma}$ are increased to $1/H_{ii}$. Note that $\underline{\alpha}, \underline{\beta}$ and $\overline{\gamma}$ have no impact on the result of case 1 and $\overline{\alpha}, \overline{\beta}, \underline{\beta}, \overline{\gamma}$ and $\underline{\gamma}$ are indifferent to the result of case 2. Fig. 16 and Fig. 17 illustrate the convergence of the total loss and minimum bus voltage magnitude under different value of $\underline{\alpha}$ for case 2. We can see decreasing the value of $\underline{\alpha}$ will improve the convergence speed of the algorithm. But when $\underline{\alpha}$ is decreased to 1, the undervoltage violations are difficult to alleviate. Therefore, it is important to tune the step sizes to proper values off-line in order to optimize the online performance of the proposed algorithm.

C. Robustness

In this subsection, we validate the robustness of our proposed voltage control algorithm against communication interruptions. The stopping criterion of the algorithm is given by $|V_i^k - V_i^{k-1}| < \epsilon$, where the tolerance ϵ is set as 1.0×10^{-4}. Assume that the communication interruptions, e.g. packet drop, occur randomly between PV systems with a probability of ρ. In case of failure in receiving the information from the neighbors for some PV systems, these PV systems would use the information obtained from last iteration. Tables III lists the average total loss and iteration number for 500 simulations under different probabilities. $\rho = 0$ represents intact communication and is the benchmark. Compare with the benchmark, the communication interruptions have limited influence on the total loss and iteration number for both cases. Therefore, the proposed DIS algorithm is robust.

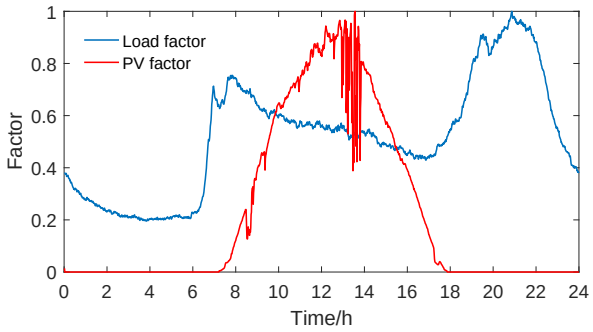

Fig. 18. Daily load factor and PV factor profiles

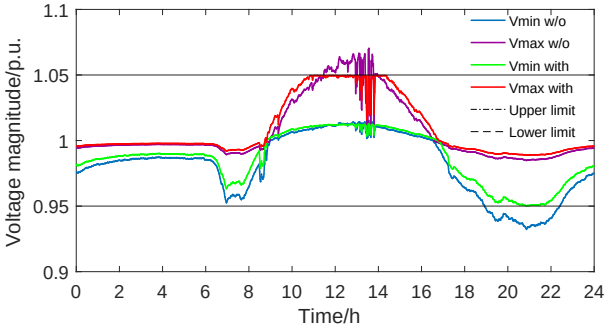

Fig. 19. Daily maximum and minimum bus voltage magnitudes with and without DIS control

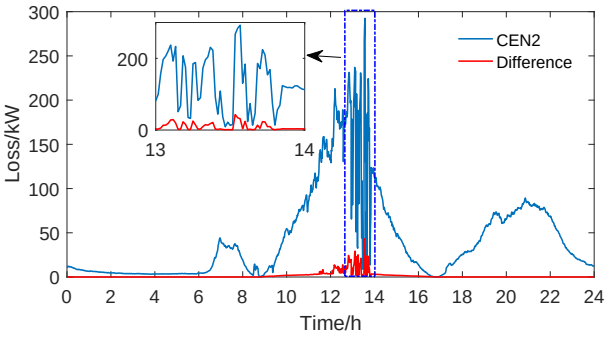

Fig. 20. Daily total loss profile of CEN2 and the difference of total loss between DIS and CEN2

D. Dynamic cases

The dynamic cases for system loading and solar energy are included to verify the effectiveness of our proposed algorithm for online application. The instantaneous maximum available PV active power and load are calculated by multiplying PV and load factors with the peak PV capacity and the peak load, respectively. Fig. 18 plots the daily load and PV factors with one-minute resolution, where the load data and solar irradiance date are obtained from [25] and [26], respectively. Since the duration of one duty cycle is four seconds, the maximum iteration number is 15 for each time interval (one minute). The step sizes and K are the same with those in subsection V-A. Fig. 19 depicts the daily maximum and minimum bus voltage magnitudes with and without DIS control. Severe overvoltage and undervoltage violations are observed without

DIS control during the peak PV period and the peak load period, respectively. As expected, all violations are eliminated by DIS control, which verifies the effectiveness of DIS for online application. Fig. 20 shows the difference of the total loss between DIS and CEN2 as well as the total loss under CEN2. The difference is relatively small and is negligible for most periods. Therefore, DIS achieves a near-optimality of CEN2 even for the dynamic cases.

VI. Conclusions and future work

In this paper, we propose a distributed online voltage control algorithm for DNs with dispersed PV systems based on dual ascent method. Different from conventional distributed algorithms, our proposed algorithm can be implemented online to address the real-time voltage fluctuation problem. At each iteration, only trivial algebraic operations are needed for the update of P-Q set-points of each PV system. Moreover, the proposed algorithm significantly lightens the communication burden such that each PV system only needs to communicate with its neighbors. Consequently, it is highly efficient for voltage control and loss minimization as the time required for completing one iteration is negligibly short. The numerical results show the voltage violations can be immediately eliminated with only one iteration and the total loss quickly converges to the near-optimality of a benchmark centralized optimization problem. The robustness of the algorithm against communication interruptions is also validated.

In this work, we assume the DN is three-phase balanced. Thus, an equivalent single-phase model is adopted. In our future work, we will extend our approach to the three-phase unbalanced DNs by considering the coupling between phases. Besides, due to the high R/X ratio of distribution lines, it is appealing to extend the current work by incorporating demand response in the future. Finally, the discrete voltage control (e.g. tapper changing) is not considered in the current work. But we will investigate the coordination between the fast responding resources (e.g. inverter-based DGs) and conventional voltage regulation devices (e.g. tapper changer and capacity banks) in the future.

Appendix

A. Proof of Proposition 1

Proof. Let $\left[\mathbf{A}^T\right]_i$ denote the i-th row of $\mathbf{A}^T$ and $\left[\mathbf{D}_r^{-1}\mathbf{A}\right]^j$ denote the j-th column of $\mathbf{D}_r^{-1}\mathbf{A}$. The entry on l-th row and j-th column of $\mathbf{D}_r^{-1}\mathbf{A}$ is $\left[\mathbf{D}_r^{-1}\mathbf{A}\right]_{lj} = A_{lj}/D_{r,ll}$. Thus, we have

$$H_{ij} = \left[\mathbf{A}^T\right]_i \left[\mathbf{D}_r^{-1}\mathbf{A}\right]^j = \sum_{l=1}^{N} A_{li}\frac{A_{lj}}{D_{r,ll}}$$

According to the definition of $\mathbf{A}$, if bus i and bus j are not directly connected, $A_{li}A_{lj} = 0, \forall\ l$ and thus $H_{ij} = 0$. □

B. Proof of Theorem 1

Proof. Since problem (27) is a strictly convex-quadratic problem with linear constraints, the Slaters condition [27] holds and thus there is no duality gap between (27) and (28). Therefore, given dual optimal solution $\mathbf{y}^*$, the primal optimal solution can be retrieved by minimizing $\mathcal{L}(\mathbf{x}, \mathbf{y}^*)$. Plugging (30) into (29), we obtain

$$\begin{aligned}\mathbf{y}^{k+1} &= \left[\mathbf{y}^k + \mathbf{D}(-\mathbf{B}\mathbf{Q}^{-1}\mathbf{B}^T\mathbf{y}^k - \mathbf{B}\mathbf{Q}^{-1}\mathbf{c} - \mathbf{b})\right]^+ \\ &= \left[\mathbf{y}^k + \mathbf{D}\nabla g(\mathbf{y}^k)\right]^+\end{aligned}$$

Thus, the iteration of $\mathbf{y}$ is based on diagonally scaled gradient projection method. To show $\mathbf{y}^k$ converges to the optimal solution $\mathbf{y}^*$, it is equivalent to show (29) is a contraction mapping regarding to the norm of the scaled error. Define $\bar{\mathbf{y}}^k = \mathbf{D}^{-\frac{1}{2}}\mathbf{y}^k$ and $\bar{\mathbf{y}}^* = \mathbf{D}^{-\frac{1}{2}}\mathbf{y}^*$. We have

$$\begin{aligned}&\left\|\bar{\mathbf{y}}^{k+1} - \bar{\mathbf{y}}^*\right\| \\ =&\left\|\mathbf{D}^{-\frac{1}{2}}\left[\mathbf{y}^k + \mathbf{D}\nabla g(\mathbf{y}^k)\right]^+ - \mathbf{D}^{-\frac{1}{2}}\left[\mathbf{y}^* + \mathbf{D}\nabla g(\mathbf{y}^*)\right]^+\right\| \\ \le&\left\|\bar{\mathbf{y}}^k - \bar{\mathbf{y}}^* + \mathbf{D}^{\frac{1}{2}}\left(\nabla g(\mathbf{y}^k) - \nabla g(\mathbf{y}^*)\right)\right\| \\ =&\left\|\bar{\mathbf{y}}^k - \bar{\mathbf{y}}^* - \mathbf{D}^{\frac{1}{2}}\mathbf{B}\mathbf{Q}^{-1}\mathbf{B}^T\mathbf{D}^{\frac{1}{2}}\left(\bar{\mathbf{y}}^k - \bar{\mathbf{y}}^*\right)\right\| \\ =&\left\|\left(\mathbf{I} - \mathbf{D}^{\frac{1}{2}}\mathbf{B}\mathbf{Q}^{-1}\mathbf{B}^T\mathbf{D}^{\frac{1}{2}}\right)\left(\bar{\mathbf{y}}^k - \bar{\mathbf{y}}^*\right)\right\| \\ \le&\left\|\mathbf{I} - \mathbf{D}^{\frac{1}{2}}\mathbf{B}\mathbf{Q}^{-1}\mathbf{B}^T\mathbf{D}^{\frac{1}{2}}\right\|\left\|\bar{\mathbf{y}}^k - \bar{\mathbf{y}}^*\right\|\end{aligned}$$

The first equality holds since $\mathbf{y}^*$ is a stationary point. The first inequality holds since the projection is non-expansive according to Proposition 1.1.4 in [22]. The second equality holds by plugging in the gradient of dual function g.

Denote $\mathbf{W} := \mathbf{D}^{\frac{1}{2}}\mathbf{B}\mathbf{Q}\mathbf{B}^T\mathbf{D}^{\frac{1}{2}}$. By definition, the Euclidean norm of $\mathbf{I}-\mathbf{W}$ equals to the largest singular value ρ of $\mathbf{I}-\mathbf{W}$. Thus, $\rho = \max_k |1-\lambda^k|$, where λ^k is k-th eigenvalue of $\mathbf{W}$. Since $\mathbf{W}$ is positive definite, $\rho < 1$ if $\lambda^{\max} < 2$, where $\lambda^{\max}$ is largest eigenvalue of $\mathbf{W}$. Therefore, (29) is a contraction mapping and $\mathbf{y}^k$ converges to dual optimal solution $\mathbf{y}^*$. Then $\mathbf{x}^k$ converges to the primal optimal solution $\mathbf{x}^*$ with $\mathbf{x}^* = -\mathbf{Q}^{-1}\mathbf{c} - \mathbf{Q}^{-1}\mathbf{B}^T\mathbf{y}^*$. □

References

[1] "US solar market insight report 2016," Solar Energy Industries Association [online]. Available: http://www.seia.org/research-resources/solar-market-insight-report-2016-year-review.

[2] C. S. Lai, Y. Jia, M. D. McCulloch, and Z. Xu, "Daily clearness index profiles cluster analysis for photovoltaic system," *IEEE Transactions on Industrial Informatics*, vol. 13, no. 5, pp. 2322–2332, 2017.

[3] Y. Li, Z. Yang, G. Li, D. Zhao, and W. Tian, "Optimal scheduling of an isolated microgrid with battery storage considering load and renewable generation uncertainties," *IEEE Transactions on Industrial Electronics*, vol. 66, no. 2, pp. 1565–1575, 2019.

[4] M. Kabir, Y. Mishra, G. Ledwich, Z. Y. Dong, and K. P. Wong, "Coordinated control of grid-connected photovoltaic reactive power and battery energy storage systems to improve the voltage profile of a residential distribution feeder." *IEEE Trans. Industrial Informatics*, vol. 10, no. 2, pp. 967–977, 2014.

[5] H. Zhu and H. J. Liu, "Fast local voltage control under limited reactive power: Optimality and stability analysis," *IEEE Transactions on Power Systems*, vol. 31, no. 5, pp. 3794–3803, 2016.

[6] E. Dall'Anese, S. V. Dhople, and G. B. Giannakis, "Optimal dispatch of photovoltaic inverters in residential distribution systems," *IEEE Transactions on Sustainable Energy*, vol. 5, no. 2, pp. 487–497, 2014.

[7] H.-G. Yeh, D. F. Gayme, and S. H. Low, "Adaptive var control for distribution circuits with photovoltaic generators," *IEEE Transactions on Power Systems*, vol. 27, no. 3, pp. 1656–1663, 2012.

[8] J. Zhang, Z. Chen, C. He, Z. Jiang, and L. Guan, "Data-driven based optimization for power system var-voltage sequential control," *IEEE Transactions on Industrial Informatics*, 2018.

[9] M. J. E. Alam, K. M. Muttaqi, and D. Sutanto, "A multi-mode control strategy for var support by solar pv inverters in distribution networks," *IEEE transactions on power systems*, vol. 30, no. 3, pp. 1316–1326, 2015.

[10] P. Jahangiri and D. C. Aliprantis, "Distributed volt/var control by pv inverters," *IEEE Transactions on power systems*, vol. 28, no. 3, pp. 3429–3439, 2013.

[11] W. Zheng, W. Wu, B. Zhang, H. Sun, and Y. Liu, "A fully distributed reactive power optimization and control method for active distribution networks," *IEEE Transactions on Smart Grid*, vol. 7, no. 2, pp. 1021–1033, 2016.

[12] C. Feng, Z. Li, M. Shahidehpour, F. Wen, W. Liu, and X. Wang, "Decentralized short-term voltage control in active power distribution systems," *IEEE Transactions on Smart Grid*, 2017.

[13] E. DallAnese, S. V. Dhople, B. B. Johnson, and G. B. Giannakis, "Decentralized optimal dispatch of photovoltaic inverters in residential distribution systems," *IEEE Transactions on Energy Conversion*, vol. 29, no. 4, pp. 957–967, 2014.

[14] K. E. Antoniadou-Plytaria, I. N. Kouveliotis-Lysikatos, P. S. Georgilakis, and N. D. Hatziargyriou, "Distributed and decentralized voltage control of smart distribution networks: models, methods, and future research," *IEEE Transactions on Smart Grid*, 2017.

[15] B. Zhang, A. Y. Lam, A. D. Domínguez-García, and D. Tse, "An optimal and distributed method for voltage regulation in power distribution systems," *IEEE Transactions on Power Systems*, vol. 30, no. 4, pp. 1714–1726, 2015.

[16] A. Maknouninejad and Z. Qu, "Realizing unified microgrid voltage profile and loss minimization: A cooperative distributed optimization and control approach," *IEEE Transactions on Smart Grid*, vol. 5, no. 4, pp. 1621–1630, 2014.

[17] A. Abessi, V. Vahidinasab, and M. S. Ghazizadeh, "Centralized support distributed voltage control by using end-users as reactive power support," *IEEE Transactions on Smart Grid*, vol. 7, no. 1, pp. 178–188, 2016.

[18] Y. Jia, Z. Xu, L. L. Lai, and K. P. Wong, "Risk-based power system security analysis considering cascading outages," *IEEE Transactions on Industrial Informatics*, vol. 12, no. 2, pp. 872–882, 2016.

[19] D. B. West *et al.*, *Introduction to graph theory*. Prentice hall Upper Saddle River, 2001, vol. 2.

[20] M. Farivar and S. H. Low, "Branch flow model: Relaxations and convexificationpart i," *IEEE Transactions on Power Systems*, vol. 28, no. 3, pp. 2554–2564, 2013.

[21] S. Boyd, N. Parikh, E. Chu, B. Peleato, and J. Eckstein, "Distributed optimization and statistical learning via the alternating direction method of multipliers," *Foundations and Trends® in Machine Learning*, vol. 3, no. 1, pp. 1–122, 2011.

[22] D. P. Bertsekas, *Nonlinear programming*. Athena scientific Belmont, 1999.

[23] N. Jaleeli, L. S. VanSlyck, D. N. Ewart, L. H. Fink, and A. G. Hoffmann, "Understanding automatic generation control," *IEEE transactions on power systems*, vol. 7, no. 3, pp. 1106–1122, 1992.

[24] D. T. F. W. Group *et al.*, "Distribution test feeders," *Available from: http://sites.ieee.org/pes-testfeeders/resources*, 2010.

[25] G. Hébrail and A. Bérard, "Individual household electric power consumption data set," *É. d. France, Ed., ed: UCI Machine Learning Repository*, 2012.

[26] "Hong Kong Observatory," [online]. Available: http://www.hko.gov.hk/.

[27] S. Boyd and L. Vandenberghe, *Convex optimization*. Cambridge university press, 2004.

Jiayong Li (S'16-M'19) received the B.Eng. degree from Zhejiang University, Hangzhou, China, in 2014, and the Ph.D. degree from The Hong Kong Polytechnic University, Hong Kong SAR, in 2018. He is currently an Assistant Professor with the College of Electrical and Information Engineering, Hunan University, Changsha, China. He was a Postdoctoral Research Fellow with The Hong Kong Polytechnic University and a Visiting Scholar with Argonne National Laboratory, Argonne, IL, USA.

His research interests include power economics, energy management, distribution system planning and operation, renewable energy integration, and demand-side energy management.

Zhao Xu (M'06-SM'12) received B.Eng, M.Eng and Ph.D degree from Zhejiang University, National University of Singapore, and The University of Queensland in 1996, 2002 and 2006, respectively. From 2006 to 2009, he was an Assistant and later Associate Professor with the Centre for Electric Technology, Technical University of Denmark, Lyngby, Denmark. Since 2010, he has been with The Hong Kong Polytechnic University, where he is currently a Professor in the Department of Electrical Engineering and Leader of Smart Grid Research Area. He is also a foreign Associate Staff of Centre for Electric Technology, Technical University of Denmark.

His research interests include demand side, grid integration of wind and solar power, electricity market planning and management, and AI applications. He is an Editor of the Electric Power Components and Systems, the IEEE PES Power Engineering Letter, and the IEEE Transactions on Smart Grid. He is currently the Chairman of IEEE PES/IES/PELS/IAS Joint Chapter in Hong Kong Section.

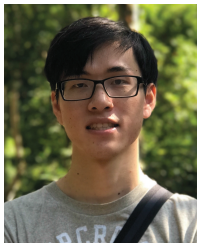

Jian Zhao (S15) received the B.Eng. degree from Zhejiang University, China, in 2013, and the Ph.D. degree from Hong Kong Polytechnic University, in 2017. He is currently with the College of Electrical Engineering, Shanghai University of Electric Power, Shanghai, China. He was a research assistant at Hong Kong Polytechnic University and a visiting scholar at Argonne National Laboratory, Argonne, IL, USA.

His research interests include distribution system operation and planning, grid integration of electric vehicles and renewable energies. Dr. Zhao was a recipient of the 2016 IEEE PES Best Paper Award.

Chaorui Zhang (S'16) received the B.Eng. degree from South China University of Technology, Guangzhou, China, in 2012, and the Ph.D. degree in Information Engineering from The Chinese University of Hong Kong, Hong Kong, in 2018. Now he is in the Hong Kong Research Center of Huawei.

His research interests focus on optimization and AI techniques in networking, such as power systems, computer networking and IOT.